Analysis of attack angle effect on flow characteristics around torpedo-like geometry placed near the free-surface via CFD

Serbest yüzeye yakın olarak yerleştirilen torpido benzeri geometri etrafındaki akış karakteristiklerine hücum açısı etkisinin CFD ile analizi

Yazar(lar) (Author(s)): Alpaslan KILAVUZ[1], Muammer OZGOREN[2], Tahir DURHASAN[3], Besir SAHIN[4], Levent Ali KAVURMACIOGLU[5], Huseyin AKILLI[6], Fuad SARIGIGUZEL[7]

ORCID[1]: 0000-0002-5180-3837   ORCID[4]: 0000-0003-0671-0890   ORCID[7]: 0000-0002-3274-7972

ORCID[2]: 0000-0002-9088-5679   ORCID[5]: 0000-0002-9981-8034

ORCID[3]: 0000-0001-5212-9170   ORCID[6]: 0000-0002-5342-7046

Analysis of Attack Angle Effect on Flow Characteristics Around Torpedo-Like Geometry Placed Near the Free-Surface via CFD

Highlights

❖ *Numerical investigation of flow structure around a torpedo-like geometry near free-surface was performed*

❖ *Interpretation of the interaction between free-surface and a torpedo-like geometry from the point of flow physics was done.*

❖ *Determination of the attack angle effect on the flow structure and drag coefficient under the influence of free-surface was carried out.*

Graphical Abstract

Flow structures of time-averaged normalized streamwise and cross-stream velocity components <u>,<v*> and streamline topology <ψ> for the angle of attack α=12° and immersion rate of h/D=1.0 at Reynolds number of Re=4x10⁴ was presented in the Figure. The free-surface effect was found to be important for lower values of immersion rate of h/D=1.0 for angle of attack α=12°. Asymmetrical flow structure, separated flow around the geometry, and introduction of air to the low-pressure flow region was occurred due to the free-surface effect. Moreover, a jet-like flow region between the geometry and the free-surface was observed at lower immersion ratios due to the restriction of flow area.*
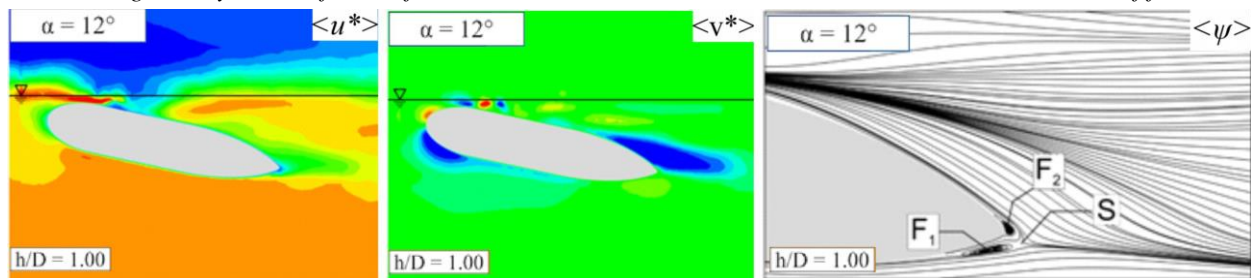

Figure. Flow structures of the $<u^*>$, $<v^*>$ and $<ψ>$ for α=12° and h/D=1.0 at Re= 4x10⁴.

Aim

The aim is to present numerically gathered data of the flow structure around a torpedo-like geometry near the free-surface at various angles of attack and immersion ratios.

Design & Methodology

In solutions, LES turbulence model was used in a 3-D flow domain containing the model at various immersion ratios and angles by defining air and water phases with VOF multiphase model. Free-surface was defined by the Open-Channel flow method at fixed heights within the flow domain.

Originality

The originality of the study comes from investigating the free-surface effect on a generalized torpedo-like geometry with given various angles of attack at immersion ratios ranging from where the model coincides/pierces the free-surface to where it is considered to be free from its influence.

Findings

A jet-like flow region was observed between the free-surface and the model at immersion ratios of h/D=0.75, 1.00, and 1.50 due to restriction of the flow area. Flow separation from the nose at increased angles of attack redirected the jet-like flow towards the sides and thus allowed the large scale vortex formations and introduced air into the wake region.

Conclusion

The wake region had an increasingly asymmetrical structure with proximity to the free-surface. The influence of the free-surface was found to be negligible in terms of time-averaged velocity components, streamline topologies, and variation of the drag coefficient at h/D≥2.50 for all cases investigated.

Declaration of Ethical Standards

The author(s) of this article declare that the materials and methods used in this study do not require ethical committee permission and/or legal-special permission.

Analysis of Attack Angle Effect on Flow Characteristics Around Torpedo-Like Geometry Placed Near the Free-Surface via CFD

(Bu çalışma ULIBTK 2019 konferansında sunulmuştur. / This study was presented at ULIBTK 2019 conference.)

Araştırma Makalesi / Research Article

Alpaslan KILAVUZ[1], Muammer OZGOREN[2*], Tahir DURHASAN[3], Besir SAHIN[1], Levent Ali KAVURMACIOGLU[4], Huseyin AKILLI[1], Fuad SARIGIGUZEL[1]

[1]Cukurova University, Engineering Faculty, Department of Mechanical Engineering, Adana, Turkey
[2]Necmettin Erbakan University, Engineering and Architecture Faculty, Department of Mechanical Engineering, Konya, Turkey
[3]Adana Alparslan Turkes University, Faculty of Aeronautics and Astronautics, Department of Aerospace Engineering, Adana, Turkey
[4]Istanbul Technical University, Department of Mechanical Engineering, Istanbul Turkey

ABSTRACT

In this study, the flow characteristics of torpedo-like geometry placed near the free-surface at various angles of attack were investigated numerically. The study was carried out at the Reynolds number of Re=4x10⁴ between immersion ratios of 0.75≤h/D≤3.5 and angles of attack α=0°,4°, 8°, and 12°. Large Eddy Simulation (LES) turbulence model was used along with the Volume of Fluid (VOF) multiphase model to investigate the effects of free-surface. Wake region had an asymmetrical structure near the free-surface as a result of the interaction. A jet-like flow region was observed between the geometry and the free-surface at lower immersion ratios due to the restriction of the flow area. This flow region had a downward movement towards the lower pressure wake region. The drag coefficient, C_D, values were increased with the decrease of immersion ratio. At angles of attack α=8° and 12°, the flow separation occurring near the nose caused an additional restriction in the flow area and directed the jet-like flow toward free-surface. Variation of Froude numbers (*Fr*) depending on the immersion ratio is examined, and it is found that *Fr* number and corresponding drag coefficient have higher values for the lower immersion ratio. The free-surface effect was found negligible at h/D≥2.5 for all cases.

Keywords: Computational fluid dynamics, drag coefficient, free-surface, LES, torpedo-like geometry.

Serbest Yüzeye Yakın Olarak Yerleştirilen Torpido Benzeri Geometri Etrafındaki Akış Karakteristiklerine Hücum Açısı Etkisinin CFD ile Analizi

ÖZ

Bu çalışmada, serbest yüzeye çeşitli hücum açılarında yerleştirilen torpido benzeri geometrilerin akış özellikleri sayısal olarak incelenmiştir. Çalışma Reynolds sayısı Re=4x10⁴'te 0.75≤h/D≤3.5 daldırma oranları ile hücum açıları α=0°,4°, 8° ve 12° arasında gerçekleştirildi. LES türbülans modeli serbest yüzey etkilerini araştırmak için Volume of Fluid (VOF) çok fazlı modeli ile birlikte kullanılmıştır. Art izi bölgesi yüzeyle etkileşimi sonucu olarak yüzeye yakın durumlarda asimetrik bir yapıya sahip olmuştur. Akış alanının kısıtlanması nedeniyle geometri ve serbest yüzey arasında daha düşük daldırma oranlarında jet benzeri bir akış bölgesi gözlemiştir. Bu akış bölgesi, düşük basınçlı art izi bölgesine doğru aşağı doğru hareketle akım yönünde ilerlemiştir. Sürükleme katsayısı, C_D, değerleri daldırma oranının düşmesi ile artmıştır. Hücum açıları α=8° ve 12° durumlarında cismin burnunun yakınında oluşan akış ayrılması akış alanında ek kısıtlamalara neden olmuş ve jet benzeri akışı serbest yüzeye doğru yönlendirmiştir. Froude sayısının daldırma oranına bağlı olarak değişimi incelenmiştir. Daldırma oranı azaldıkça Froude sayısı buna karşılık gelen sürüklenme katsayısı da artmaktadır. İncelenen tüm akış özellikleri serbest yüzey etkisinin h/D≥2.5'te ihmal edilebilir mertebede olduğunu göstermektedir.

Anahtar Kelimeler: Hesaplamalı akışkanlar dinamiği, LES, serbest-yüzey, sürüklenme katsayısı, torpido benzeri geometri.

1. INTRODUCTION

Underwater vehicles are used in many fields from scientific fields such as an archeological and geological survey to underwater defense in the navy. While the manned vehicles offer substantial control and observation opportunities, unnamed underwater vehicles offer the ability to submerge deeper, higher velocities, high maneuverability and camouflage surrounding environment to track marine life with the elimination of design requirements coming from having an operator

*Sorumlu Yazar (Corresponding Author)
e-posta : mozgoren@gmail.com

inside the vehicle. Underwater vehicles share a common cylindrical hull design among themselves with varying nose shaped and trailing edge shapes with or without wing-like appendages. The design of underwater vehicles which can travel more distances with a limited amount of fuel or inertia, or which can travel short distances with high maneuverability at a short time depending on the understanding of flow characteristics around these bodies. For instance, when fuel efficiency is desired, the drag coefficient should be as low as possible and when the maximum control is desired for purposes such as using a camera to capture marine life, fault line, or shipwreck for archeological purposes, minimum noise and maximum control must be achieved through the study of hydrodynamic characteristics and adding appropriate devices. Givler et al. [1] studied the wake of a submarine using the finite element method at $Re=1.2x10^7$ by utilizing the k-ε RANS turbulence model. Reichl et al. [2] investigated the wake of a cylinder near the free-surface. They carried out their investigation at low Froude numbers for different immersion ratios and reported significant changes in the Strouhal number, St, as the immersion ratio was changed. At h/D=0.70, St had its peak value. They observed a reduction in the lift force as a result of jet-like flow occurred between the geometry and the free-surface. Evans and Nahon [3] studied hydrodynamic forces at increasing angles of attack of an autonomous underwater vehicle (AUV). Alvarez et al. [4] researched the optimum hull design of an underwater vehicle near the free-surface. They utilized the first-degree Rankine panel method to observe the wave resistance near the free-surface. They managed to reduce overall drag resistance by 25% at increasing Froude numbers by determining an optimum shape. Jagadeesh and Murali [5-6] experimentally and numerically studied the effect of free-surface on the hydrodynamic coefficients of a non-symmetrical AUV using a towing tank-based experiment and RANS turbulence models in CFD at a larger range of Reynolds numbers. They evaluated various RANS turbulence models near the free-surface they simulated using the Volume of Fluid (VOF) multiphase model. Their study was carried out between the Reynolds numbers $Re=2.12x10^5$ to $7.42x10^5$ and between the immersion ratio from h/D =0.75 to 4. They also varied the angle of attack between α=0° and 15° with increments of 5°. After comparing the results with the experimentally obtained results ranging between Reynolds numbers $Re=1.05x10^5$ to $3.67x10^5$, they reported that the k-ε realizable RANS model was more successful. Ozgoren et al. [7] experimentally investigated the interaction between a sphere and free-surface with PIV and dye experiments for various immersion ratios at 2500≤Re≤10000. They reported that the wavy flow structure formed due to the flow separation from the part of the sphere submerged in the water exhibits a very complex flow structure. The immersion ratio for h/D=0 indicates that the reunification of the separated flow from the surface is approximately 1.9D from the base of the sphere. This situation is up to h/D=0.50 and higher

immersion ratios of 1≤h/D≤2 separated flow area is dampened to the current direction without joining the surface, and then reported that it reached the free-stream conditions. Hassanzadeh et al. [8] utilized the LES turbulence model to numerically study the hydrodynamic coefficients and flow characteristics of a sphere in the wake region under the effect of the free-surface at h/D=0.25, 0.5, 1, and 2 immersion ratios at $Re=5x10^3$. They reported that the influence of the free-surface decreases as the immersion ratio is increased. Dogan et al. [9] researched the flow structure of a sphere and its interaction with the free-surface experimentally. They carried out experiments in an open water channel for three different spheres with a smooth surface and passive flow control applied under the influence of free-surface flow. During their studies, they varied the Reynolds number between 2500≤Re≤10000 and the immersion ratio varied between 0.25≤ h/D≤3. It is reported that at an immersion ratio of h/D=2 flow characteristics were similar to uniform flow conditions. Nematollahi et al. [10] numerically examined the influence of free-surface on the flow around an underwater vehicle using VOF multiphase model at different immersion ratios and found that the VOF model was sufficient to simulate the interaction between geometry and free-surface. Goktepeli et al. [11] carried out experimental studies using PIV measurements to investigate the flow structure around torpedo-like geometry under the influence of free-surface. They stated that as the immersion ratio decreases, the flow structure changes drastically. Salari and Rava [12] studied the hydrodynamics of an autonomous underwater vehicle numerically by employing the k-ω and k-ε turbulence models. They performed the study at various Froude numbers and for submergence depth ratios of 0.75 D, 1 D, 1.5 D, 2D, and 4 D. They stated that the free surface of water affects the drag coefficient of the vehicle and that this effect depends on its submergence depth and speed. Also, they observed that the drag near the free surface is larger than the drag at greater depths (h/D >3) and that the flow structure becomes asymmetric as the vehicle moves toward the free surface of the water. Javanmard et al. [13] performed numerical simulations to investigate the drag coefficients of an AUV under the effect of struts and free surface. They carried out the simulations for various submergence depth ratios and for Reynolds numbers of $1.9x10^6$ and $3.16x10^6$. Their results showed that the drag coefficient value of the AUV is reduced with the existence of struts and that the amount of reduction depends on the submergence depth, and Reynolds number. Tian et al. [14] studied the effect of free surface waves on the hydrodynamic performance of an autonomous underwater vehicle numerically. They carried out the simulations by utilizing the k-ω SST turbulence model along with the VOF multiphase model which is provided by the ANSYS-FLUENT software. They found that the wave height affects the lift force of the vehicle significantly and that the drag coefficient increases as the submergence depth is decreased. Kilavuz [15] studied the

effect of free-surface on various flow characteristics. He reported that C_D was increased with decreasing immersion ratios. He observed that the vortex shedding frequency and the Strouhal numbers for geometries placed at an angle of attack α=0° were significantly changed at Re=2x10⁴ increasing with the decrease of immersion ratios, however, for Re=4x10⁴, the values of St varied slightly with a similar trend. The present study has been presented in the 22nd Congress on Thermal Science and Technology [16].

The examined studies in the literature have different geometries from the present study. This study has been focused on the CFD analysis to yield the free-surface effects on the flow characteristics around a torpedo-like geometry.

2. MATERIAL AND METHOD

There are many methods to determine turbulence viscosity in numerical studies. In this study, the flow structure around the investigated model is evaluated by using the Large Eddy Simulation (LES) turbulence model. The LES turbulence model uses equations that characterize the length of a large-scale vortex as the basis [17]. Navier-Stokes and continuity equations are the general equations used in fluid mechanics and they are also the basis of turbulence models. Continuity for incompressible flow and the Navier-Stokes equation:

$$\frac{\partial \overline{u_i}}{\partial x_i} = 0 \tag{1}$$

$$\frac{\partial \overline{u_i}}{\partial t} + \frac{\partial \overline{u_i u_j}}{\partial x_j} = \frac{1}{p}\frac{\partial \overline{p}}{\partial x_i} - \frac{\partial \tau_{ij}}{\partial x_j} + v\frac{\partial^2 \overline{u_i}}{\partial x_i \partial x_j} \tag{2}$$

where u_i is a filtered velocity component through Cartesian x_i coordinate, u_j is a filtered velocity component though x_j coordinate and p is the fluid pressure. LES turbulence model enables the separation of large and small-scale eddies from each other through filtration. In the spatially filtered Naiver-Stokes equation, the sub-grid scale (SGS) stress is given by Equation 3. In this equation, the effect of small-scale eddies on larger scaled eddies for a small-scaled stress tensor is determined as:

$$\tau_{ij} = \overline{u_i u_j} - \overline{u u} \tag{3}$$

The eddy-viscosity type SGS models are given as:

$$\tau_{ij} - \frac{1}{3}\tau_{kk}\delta_{ij} = -2\mu_t \overline{S_{ij}} \tag{4}$$

where τ_{kk} is the strain residuals in a subgrid-scale. In a subgrid-scale, turbulent viscosity is symbolized with μ_t and S_{ij} is the rate of strain tensor computed from the resolved scales.

VOF model uses the following equation:

$$\frac{1}{p_q}\left[\frac{\partial}{\partial t}\left(\alpha_q p_q\right) + \nabla * \left(\alpha_q p_q\ \vec{v}_q\right) = S_{\alpha q} + \sum_{p=1}^n\left(\dot{m}_{pq} - \dot{m}_{qp}\right)\right]$$

Where $\dot{m}_{qp}$ is the mass transfer from phase q to phase p and $\dot{m}_{pq}$ is the mass transfer from phase p to phase q. The volume fraction is not solved for the primary phase; the primary-phase volume fraction is based on the following constraint:

$$\sum_{q=1}^n \alpha_q = 1 \tag{6}$$

The volume fraction equation may be solved either by using implicit or explicit time discretization. The Implicit scheme equation used in this study is given as:

$$\frac{\alpha_q^{n+1}p_q^{n+1} - \alpha_q^n p_q^n}{\Delta t}V + \sum_f\left(p_q^n U_f^{n+1}\alpha_{q,f}^{n+1}\right) = \left[S_{\alpha q} + \sum_{p=1}^n\left(\dot{m}_{pq} - \dot{m}_{qp}\right)\right]V$$

where n+1 is the current time step, n is the previous time step, $\alpha_{q,f}$ is the face value of the qth volume fraction, V is the volume of cell and U_f is the flux through the face, based on normal velocity [18].

Flow characteristics around the torpedo-like geometry model have been investigated at various angles of attack. The obtained results have been compared at each immersion ratio h/D for each angle of attack α=0°, 4°, 8° and 12° at the immersion ratios of h/D= 0.75, 1.0, 1.5, 2.0, 2.5, 3.0 and 3.5 at the Reynolds number Re=4x10⁴. The Reynolds number was calculated using the characteristic length as Re=(ρU∞L)/μ. Here, L is the length of the model, ρ is fluid density, μ is the dynamic viscosity and U∞ is the free-stream velocity. The length was taken as   L = 200 mm and the diameter was taken as D = 40 mm and the free-stream velocity was taken as U∞ = 200 mm/s. The 3-D volume with the following distances relative to the model as presented in Figure 1a was used in this numerical study.

The torpedo-like geometry has been designed similar to the studies of Myring [19], Barros et al. [20], Gao et al. [21], Sousa et al. [22], Alam et al. [23] by using Myring Equations. The features of Myring equations were formed of a nose, a middle body cylindrical, and a tail section. The nose section is characterized by the variation of semi-elliptical radius distribution as follows:

$$r_1(x) = \frac{1}{2}D\left[1 - \left(\frac{x-a}{a}\right)^2\right]^{1/n} \tag{8}$$

and the tail section is defined by the cubic relationship:

$$r_1(x) = \frac{1}{2}D - \left[\frac{3D}{2c^2} - \frac{tg\theta}{c}\right](x-a-b)^2 + \left[\frac{D}{c^3} - \frac{tg\theta}{c^2}\right](x-a-b)^3$$

In these equations, x is the axial distance from the beginning and end of the nose and tail, respectively. As shown in Figure 1b, the particular dimensions nose length, middle body length, tail length, diameter, bare hull length, Myring angular parameter, and potential parameter of torpedo-like geometry in the presented study were respectively identified as a=40mm, b=80mm,

c=80mm, D=40mm, L=200mm, θ=~30°, and n=2. The selection of these values of the nose and tail parameters was based in previous studies in the literature Myring [19], Barros et al. [20], Gao et al. [21] Sousa et al. [22], Alam et al. [23]. Considering the bare hull lengths and diameter, the length of each section, nose, middle, and tail, were calculated from equations 8 and 9.
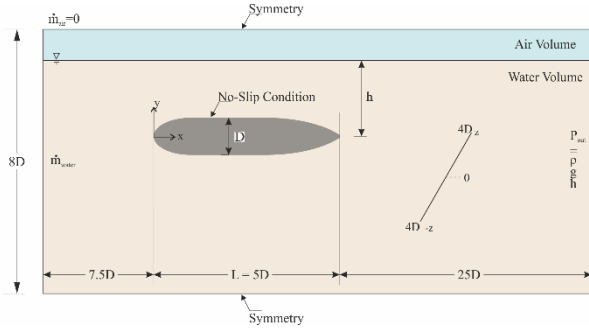

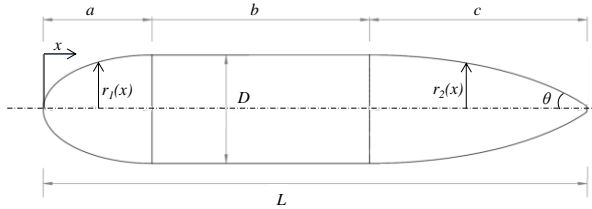**Figure 1a.** Generated flow domain.

Figure 1b. Geometric parameters of torpedo-like geometry with respect to the Myring Equations.

Mesh generation was done separately for three prismatic volumes surrounding the surface of the model. Created tetrahedral cells have been transformed into polyhedral cells using FLUENT as they can be seen in Figure 2.
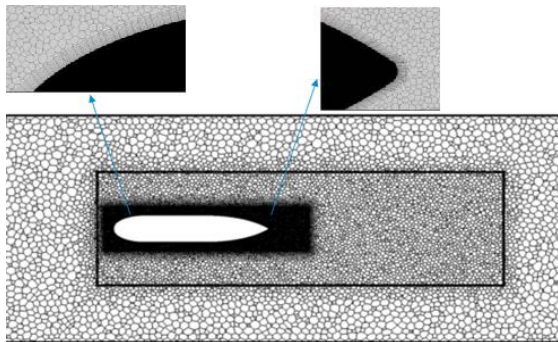

Figure 2. Designed grid structure around a torpedo-like geometry

The main advantage of polyhedral mesh is that there are many neighbors in each cell, so the gradients can be well approximated. Polyhedral cell structure is also less susceptible to stretching than the tetrahedron structure, resulting in higher mesh quality and improved stability of numerical solutions. Compared to tetrahedral and hybrid mesh structures polyhedral meshes have 3 to 5 times lower number of total cells which leads to faster converge

of residuals with fewer iterations resulting in significantly lower solution times as stated by ANSYS [24].

As a result, an average value of non-dimensional wall distance y^+_{avg}=0.82 has been achieved. From the law of the wall, y^+ is given as $y^+ = \frac{yu_*}{v}$ where u_* is friction velocity, y is the absolute distance from the wall and v is the kinematic viscosity. The value of y^+ indicates the location of the cell closest to the wall in a given flow. The value of $y^+<5$ indicates that the cell is within the viscous sublayer, $5<y^+<30$ indicates the cell is in the buffer layer and $y^+>30$ indicates that the cell is within the logarithmic layer [25]. In LES turbulence model, $y^+_{avg} = 1$ is desired as it is explained by ANSYS [24].

Mesh independence was also achieved upon observing the drag coefficient using larger and finer mesh structures resulting in various numbers of cells. Table 1. Displays the change of obtained C_D values with the number of cells within the flow domain. Change of C_D between 34.2 million and 11.6 million cells was found to be about 1.45% and compared to their computational costs, the study was continued using 11.6 million cells with element sizes of 0.001 to 0.005 and 0.01 mm expanding further away from the surface of the model.

Table 1. Study of mesh independence using different cell-sized domains for h/D=3.5 and α=0°.

Tetrahedral Cells	Polyhedral Cells	C_D
2,500,000	550,000	0.1965
6,000,000	1,265,000	0.1889
11,600,000	2,500,000	0.1788
34,200,000	7,420,000	0.1762

In order to examine the influence of free-surface, one of the sub-models of the VOF multiphase model, Open-Channel flow was used to define the free-surface height at every immersion rate whilst the model was kept stationary inside the flow domain. The implicit scheme was preferred due to its highly robust design. Inlet and outlet surfaces were retained as one segment rather than the traditional way of separating each of them for each fluid by utilizing the ability of Open-Channel flow to separate fluids at inlet and outlet surfaces for initialization after defining the height of the free-surface from the bottom of the flow domain. The Courant–Friedrichs–Lewy (CFL) condition ($C = \frac{u\Delta t}{\Delta x} \leq 1$) where C is the Courant Number, u is the velocity, Δt is the time step and Δx is the length interval, was satisfied the recommended value of $C \leq 50$ by the ANSYS for implicit scheme solvers. The time step size was taken as $\Delta t = 0.068s$ [26-27].

3. RESULTS AND DISCUSSION

3.1. Flow Structure

Flow structures around the torpedo-like geometry were examined at $Re=4 \times 10^4$ and increasing immersion ratios of h/D and compared side by side with increasing angle of attack $\alpha=0°$, $4°$, $8°$, and $12°$ at immersion ratios of h/D= 0.75, 1.00, 1.50 and 2.50 where the results showed the most distinguishable flow structures. Results are given as time-averaged normalized streamwise velocity component $<u^*=u/U_\infty>$, time-averaged normalized cross-stream velocity component $<v^*=v/U_\infty>$ and time-averaged streamline topologies $<\psi>$ around the model. The values of the drag coefficient are also given both graphically and numerically comparing the effect of angle of attack at each immersion ratio. The time-averaged streamline topology has a rotational flow structure near the stern of the torpedo-like geometry. Here, F represents the focus of the rotational flow and S denotes the saddle point of the flow structure where the u and v components of the velocity become zero. The location of the F and S depends on the pressure values in the flow field. Rotational flow occurs from the higher pressure flow region to the lower one in the edge of the stern. The velocity gradient in the near wake region of the geometry increases and thus rotational flow region including focus and saddle point appears. Those are the critical point of the flow structure from the point of flow physics and they can be used comparison parameters between computational fluid dynamics and experimental studies.

Figure 4 and Figure 5 show the effect of the angle of attack on the streamwise velocity distribution. These contours show that the streamwise velocity increases between the model and free-surface relative to the lower part of the model. Water flow accelerating through the restricted flow area between the upper surface of the model and the free-surface creates a jet-like flow region. This jet-like flow is directed downwards towards the wake region with the lower pressure and it can be observed from Figure 6 and Figure 7. Small clustered areas with high magnitudes of cross-stream velocity near the free-surface indicate the surface deformation. An asymmetrical wake structure tented away from the free-surface can be seen for $0.75 \leq h/D \leq 1.50$ at $\alpha=0°$ with the presence of this jet-like flow from the free-surface. The time-averaged streamlines presented in Figure 8 and Figure 10 also show this asymmetrical wake structure, jet-like flow sweeping the rear section of the model at h/D=0.75 eliminating the large-scaled vortex formations. At h/D=2.50, as it can be seen from the absence of the jet-like flow and the smaller area with downward movement on the upper surface of the rear section along with the closer position of the saddle point compared to h/D=1.50, the effect of free-surface is negligible.

At the angle of attack $\alpha=4°$, due to the additional restriction of the flow area and flow separation near the nose, the jet-like flow is directed around the model at h/D=0.75. Due to this behavior, the jet-like flow no longer sweeps the upper surface of the stern section as it can clearly be seen from streamwise velocity contours and streamlines. The wake region is directed towards the free-surface and is slightly larger than the wake observed at $\alpha=0°$. At h/D=1.00, the jet-like flow having larger magnitudes of velocity due to additional restriction can be seen to be directed towards the free-surface after interacting with the flow separation near the nose of the model. Streamlines show the dramatic size increase of the wake region compared to $\alpha=0°$. However, at h/D=1.50 as a result of the angle of attack having $\alpha=4°$ inclination the model interacts more with the free-surface and then the wake region becomes significantly smaller when compared to $\alpha=0°$ case. At h/D=2.50 similar to $\alpha=0°$ the effect of free-surface is negligible as the model no longer interacts with the free-surface.

For the case of $\alpha=8°$ at h/D=0.75, the nose of the model directs the incoming flow towards the sides. The lack of downward moving flow coming from free-surface causes the wake to be directed towards free-surface and allows the formation of large-scale vortex structures. At h/D=1.00, the jet-like flow connects with the upper surface of the geometry after the restriction of the flow separation and sweeps the upper surface of the rear section preventing large-scale vortex formation similar to $\alpha=0°$ and $4°$ cases. At increased immersion ratios flow structure is similar to $\alpha=4°$.

The nose of the model pierces the free-surface at $\alpha=12°$ for the immersion ratio of h/D=0.75. Surface piercing along with the occurrence of flow separation earlier compared to $\alpha=8°$ causes a significantly longer and wider wake region with the downward moving flow area tended towards the free-surface instead of sweeping the stern section. Flow structure at increased immersion ratios is similar to $\alpha=4°$ and $8°$ with a larger wake.

For all angles of attack investigated it can be said that as the angle of attack was increased, more of the jet-like flow was directed towards the sides of the model diminishing its ability to prevent large-scale vortex formations. While the wake structures of inclined models were similar, saddle point moved closer to the trailing edge. Foci points showing the formation of trapped vortices within the circulating region also moved closer to the stern section.

3.2. Drag Coefficient

Table 2 and Figure 3 show the variety of drag coefficient C_D with immersion ratios for each angle of attack. The peak drag coefficient values for each angle of attack were obtained at the smallest immersion ratio of h/D=0.75. At $\alpha=12°$ early flow separation combined with the additional flow, restriction caused a smaller change at h/D=1.00 meanwhile, other cases resulted in significantly lower drag coefficients. The high values of C_D at lower immersions can be explained by the jet-like flow causing the air above to free-surface to enter the wake region thus creating a lower pressure overall behind the trailing edge. From the trend, it can be said that the

effect of free-surface lasts up to h/D<2.5 for all angles of attack.

3.3. Effect of Froude Number

In open water channel studies, the effect of free surface on flow characteristics of the immersed bluff body is substantially important. In these cases, the wave propagation and the interaction of the free-surface with the investigated object become significant. The Froude number, $Fr = U_\infty / \sqrt{gh}$ shows the ratio of inertial force to hydrostatic force. In this study, the model was held stationary utilizing the open-channel flow multiphase sub-model. Thus, free-surface height was changed for each immersion ratio instead. Table 3 and Figure 9 present the variation of the Froude number based free-surface height with immersion ratios, h/D.

When the Froude number, *Fr* is calculated using the distance between the free-surface center of the model instead of the height of the free-surface a relation between Froude number, *Fr*, and the drag coefficient C_D was obtained as represented in Figure 11. For the immersion ratios of 2.0≤h/D≤3.5, the ratio of Froude numbers to drag coefficients remains approximately constant however it can be seen that the effects of the free-surface on the drag coefficient, C_D increase at higher Froude numbers, *Fr*. The trend is similar to the trends free-surface wave resistance coefficient, C_W against the

Froude number found in the literature for subcritical Froude numbers *Fr*≤1 [28-29]

Table 2. Drag coefficients for investigated cases

h/D	α=0°	α=4°	α=8°	α=12°
0.75	0.3524	0.3571	0.4706	0.4815
1.00	0.2456	0.2662	0.3285	0.4711
1.50	0.1928	0.1974	0.2268	0.2961
2.00	0.1929	0.2135	0.2423	0.3107
2.50	0.1759	0.1858	0.2187	0.2800
3.00	0.1734	0.1858	0.2262	0.2877
3.50	0.1788	0.1924	0.2253	0.2915

Table 3. Variation of Froude numbers calculated from the freesurface height, h with immersion ratios h/D.

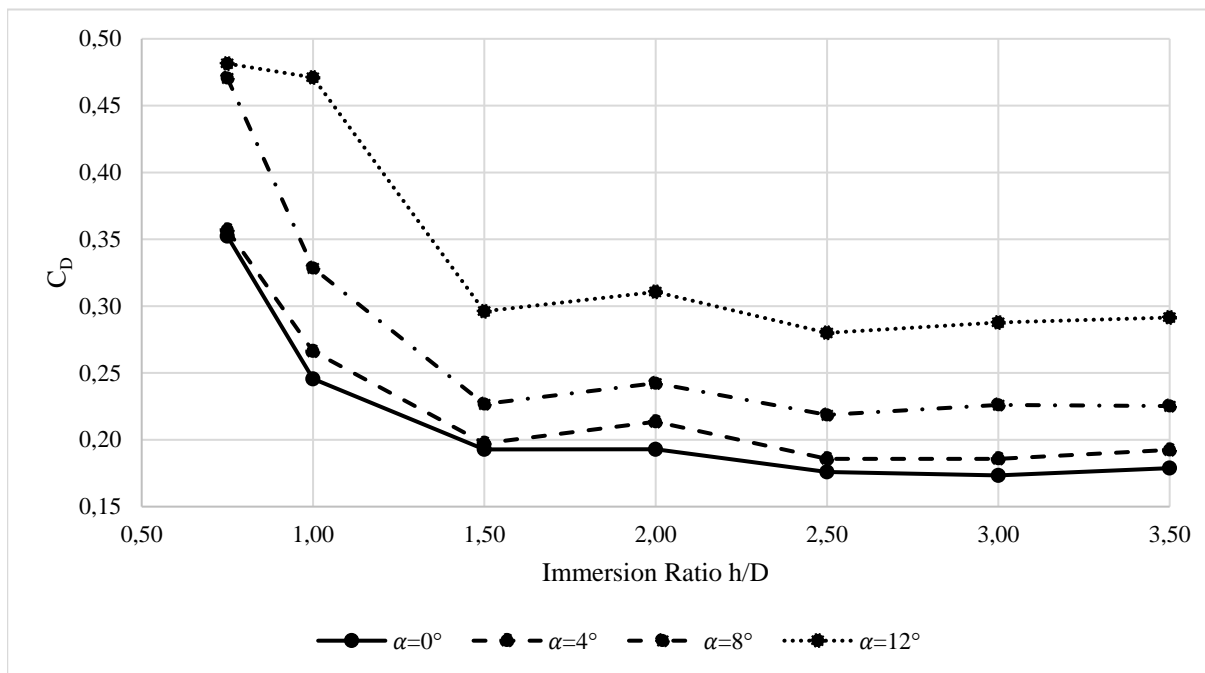| Immersion ratio (h/D)	Froude number (Fr)
0.50	0.1505
0.75	0.1465
1.00	0.1428
1.00	0.1361
2.00	0.1303
2.50	0.1252
3.00	0.1207
3.50	0.1166

Figure 3. Variations of drag coefficient C_D with the angle of attack α and immersion ratio h/D
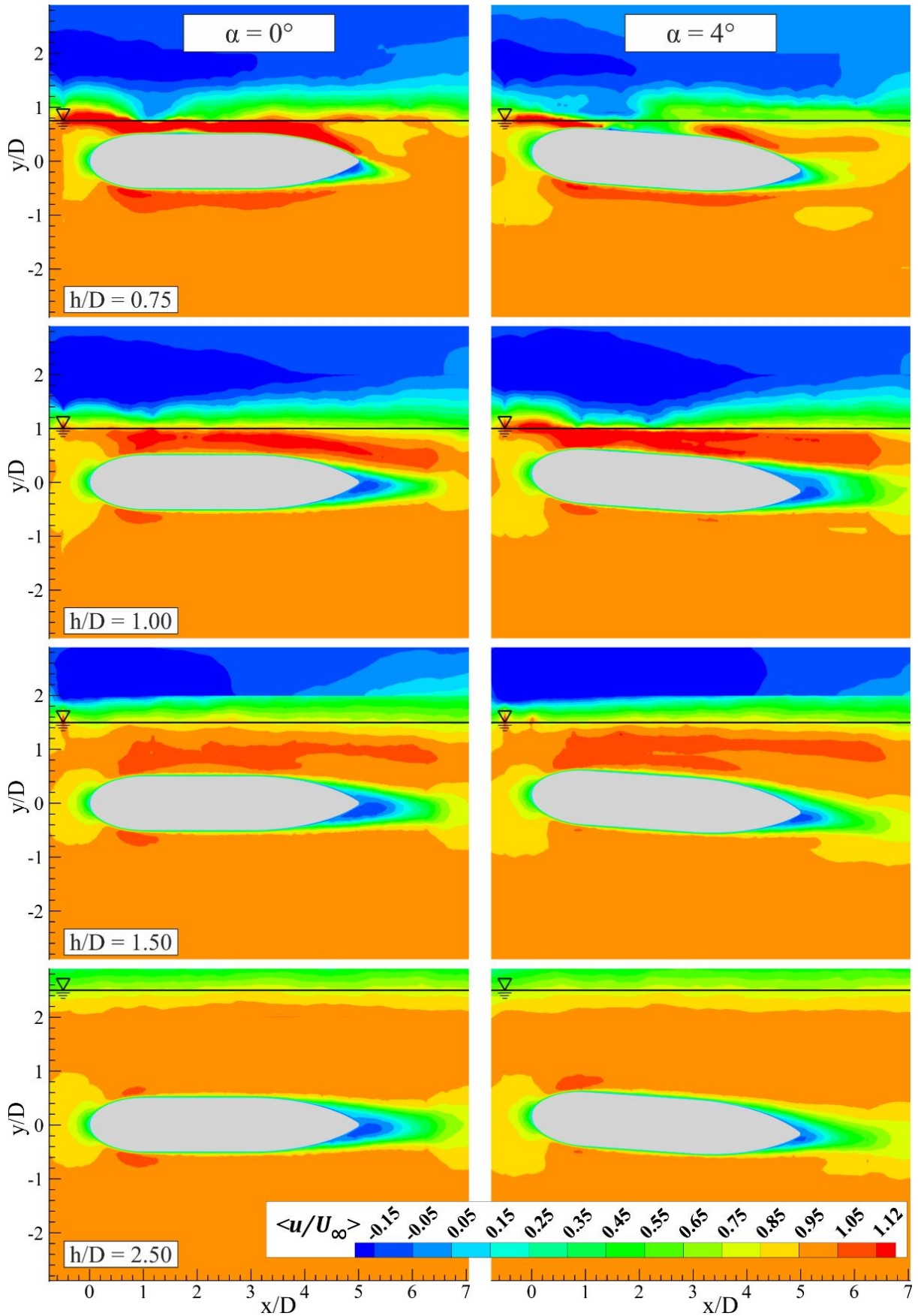
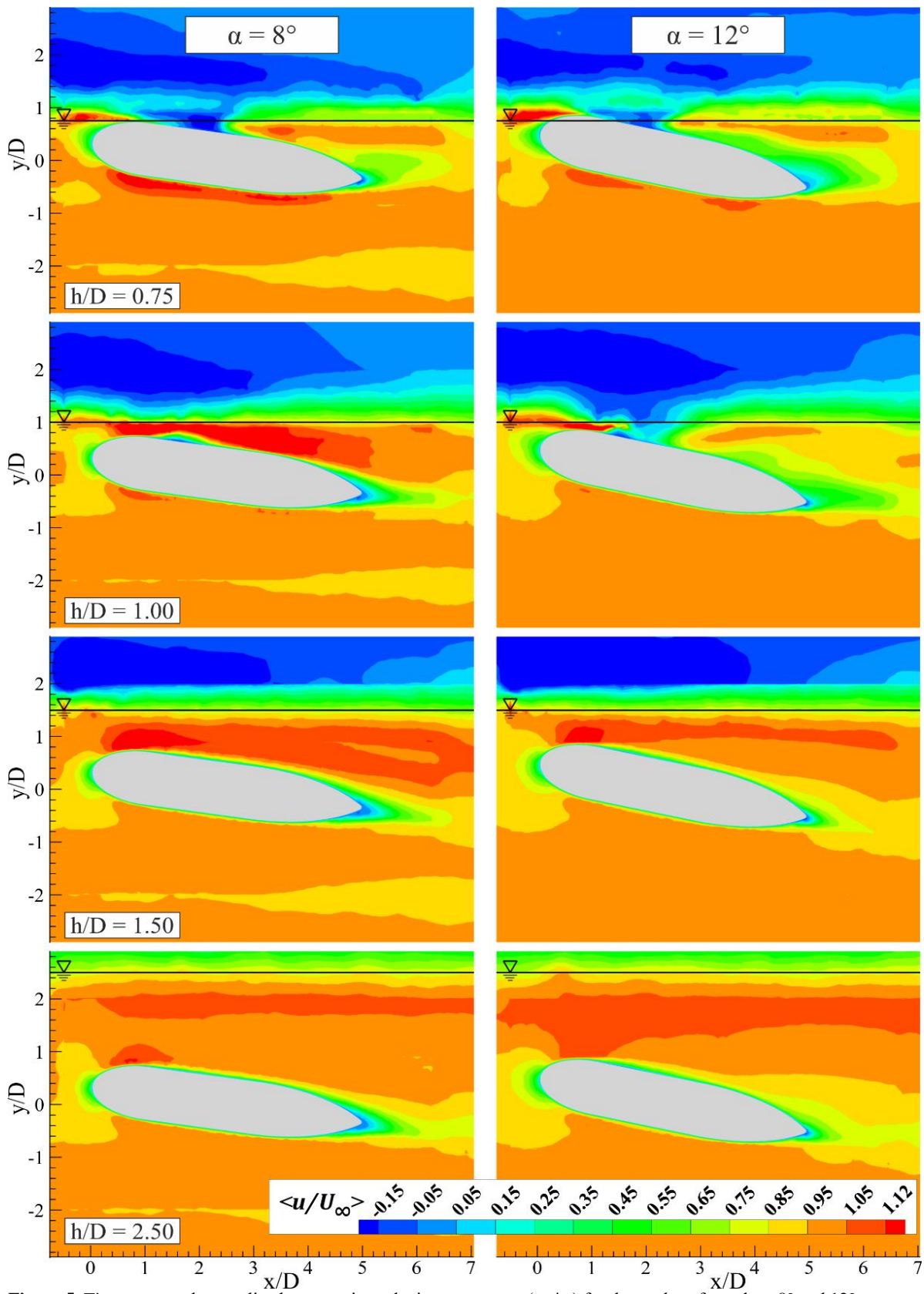**Figure 4.** Time-averaged normalized streamwise velocity component (<u*>) for the angles of attack α=0° and 4°

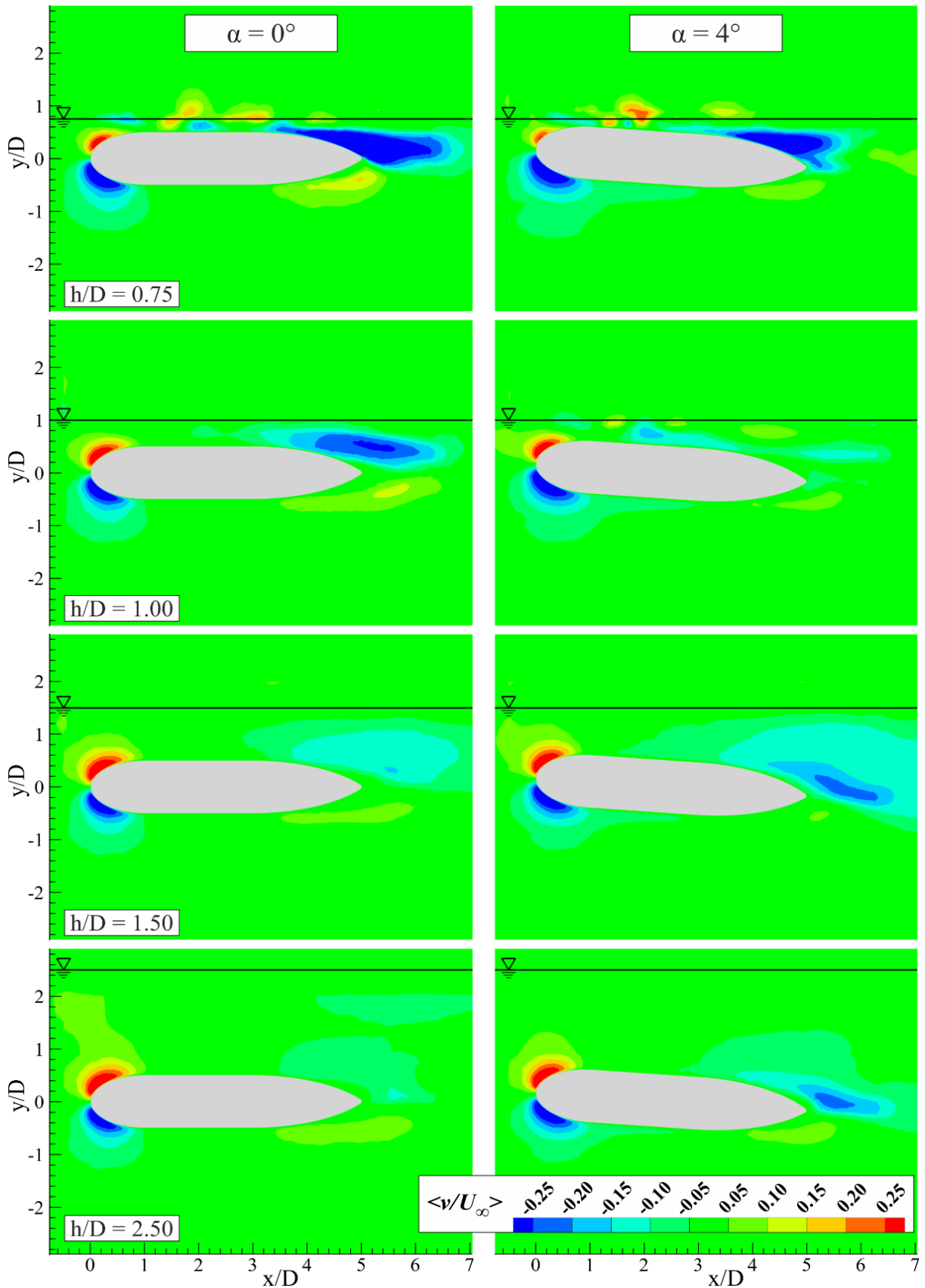**Figure 5.** Time-averaged normalized streamwise velocity component (<u*>) for the angles of attack α=8° and 12°

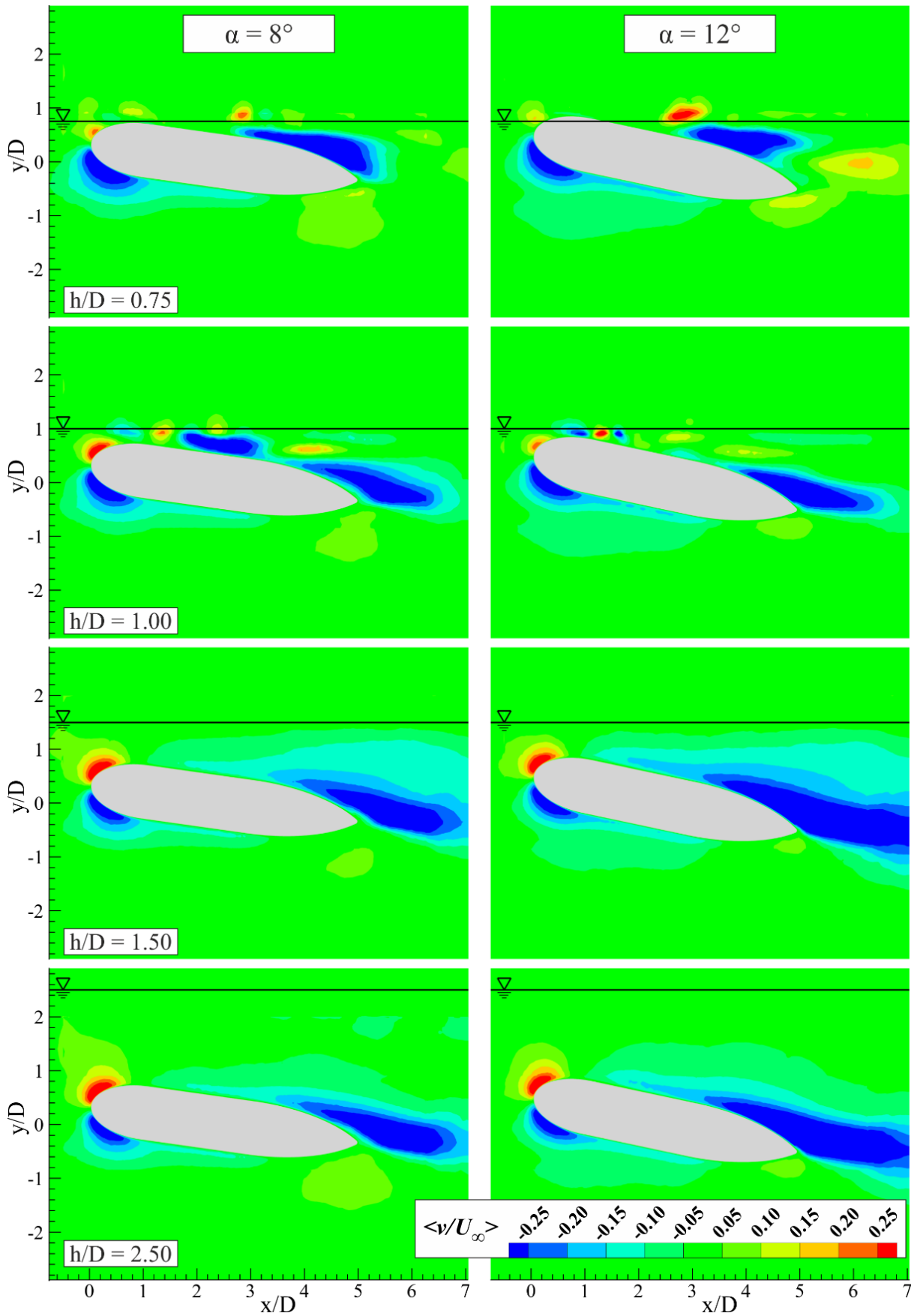**Figure 6.** Time-averaged normalized cross-stream velocity component (<v*>) for the angles of attack α=0° and 4°

Figure 7. Time-averaged normalized cross-stream velocity component (<v*>) for the angles of attack α=8° and 12°
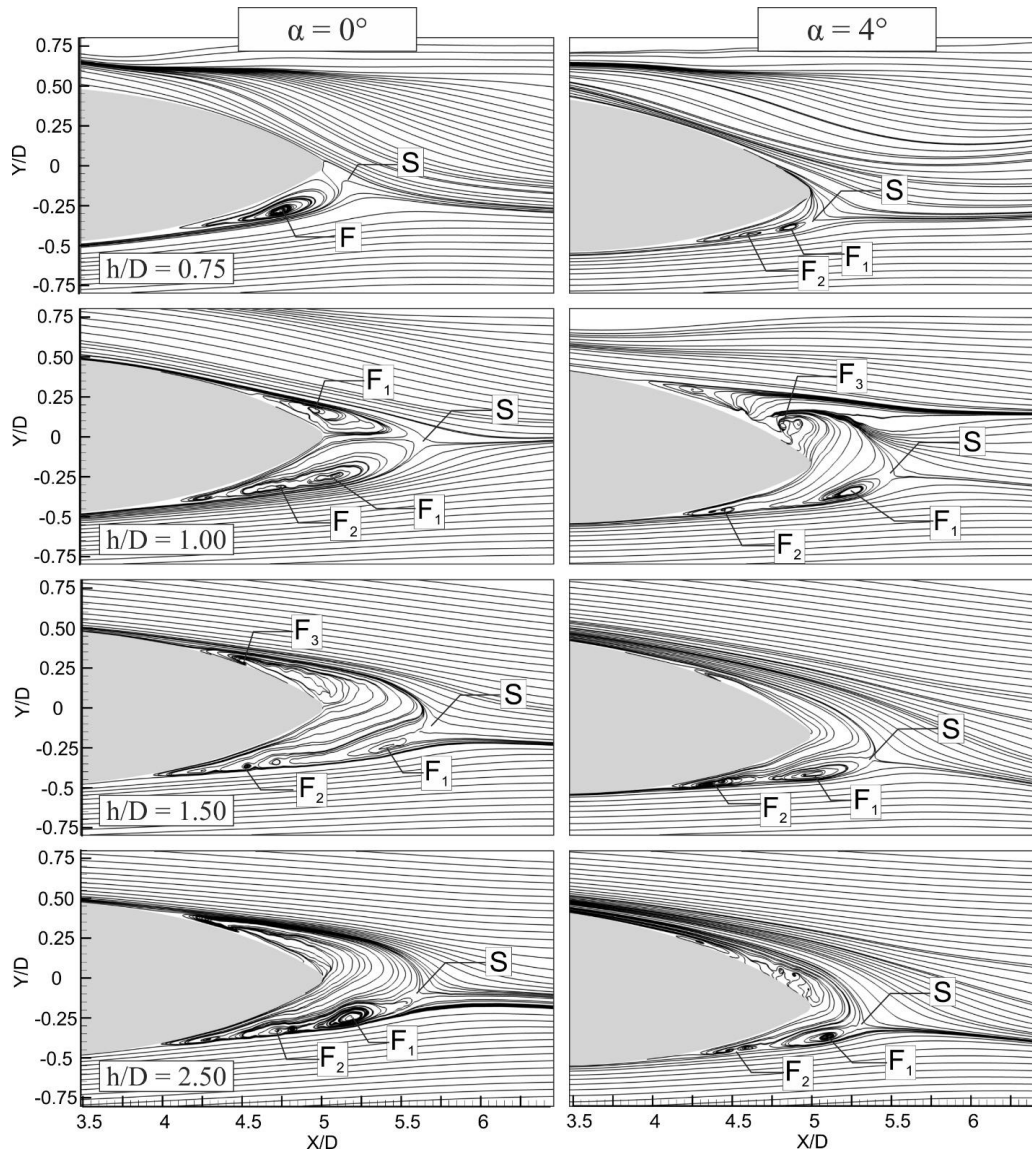
Figure 8. Time-averaged streamline topologies $\langle\psi\rangle$ for the angles of attack $\alpha=0°$ and $4°$
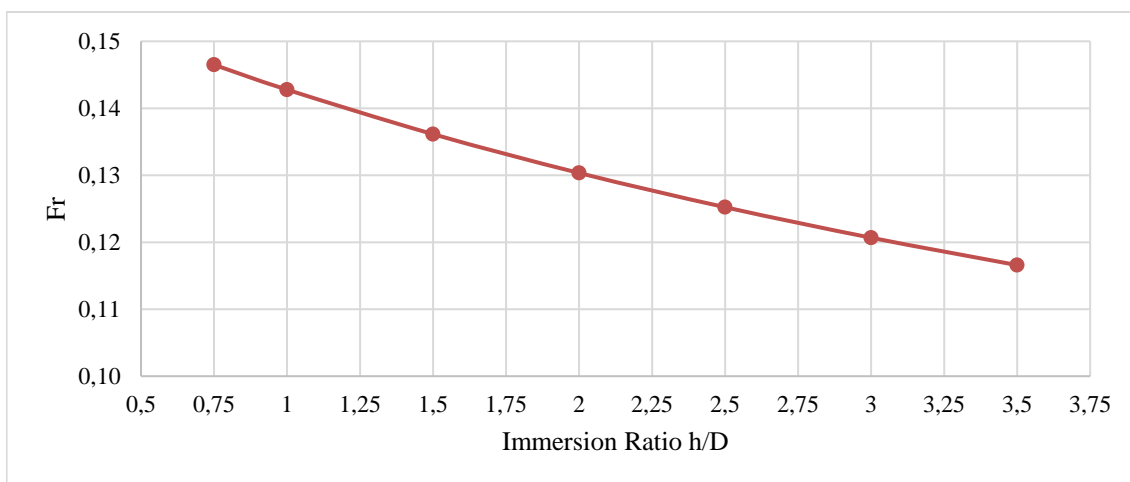

Figure 9. Variation of the Froude number calculated from free-surface height with the immersion ratios
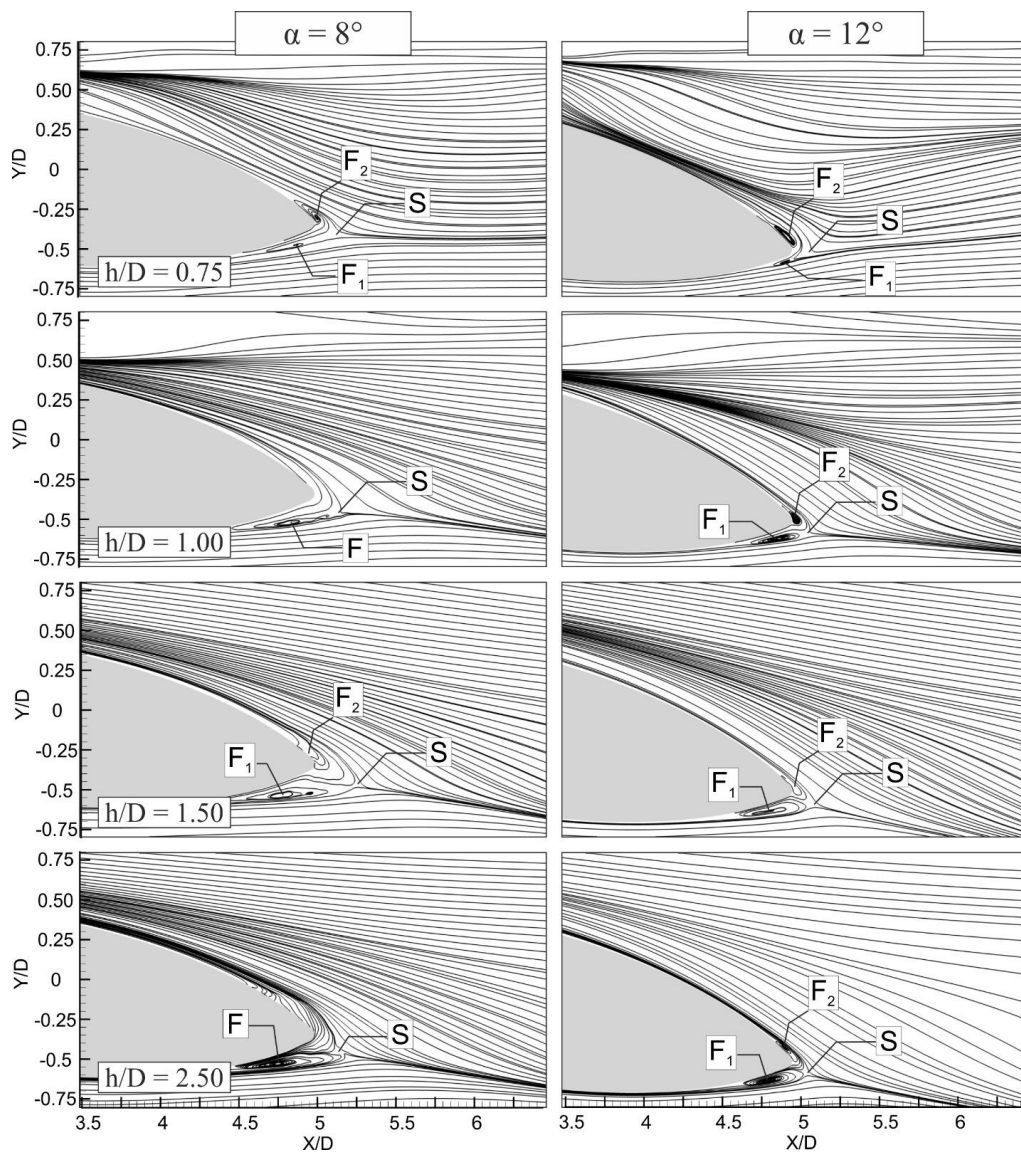
Figure 10. Time-averaged streamline topologies $\langle\psi\rangle$ for the angles of attack $\alpha=8°$ and $12°$
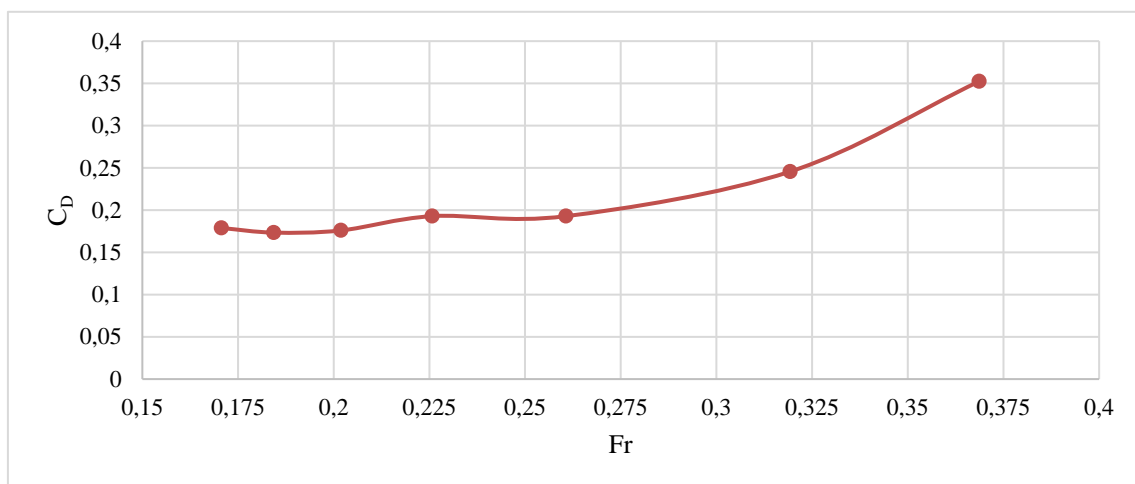

Figure 11. Variation of Froude number calculated from the submergence location of the torpedo-like geometry to the free-surface with the drag coefficient

4. CONCLUSION

Flow characteristics around the torpedo-like geometry were investigated numerically using LES at increasing immersion ratios h/D=0.75, 1.00, 1.50, 2.00, 2.50, 3.00 and 3.50 for increasing angles of attack of α=0°, 4°, 8°, and 12° at Re= 4x10^4.

Near-symmetrical flow structure was observed for the model at h/D = 2.5 and α=0°. The asymmetry of the wake structure was increased as the angle of attack was decreased, and the immersion ratio was decreased. Time-averaged normalized streamwise and cross-stream velocity components showed that a jet-like flow region occurred due to the restriction of the flow area. This flow region affected the vortex formation with its high magnitudes of downward movement around the trailing edge, preventing large-scale vortex formation on the upper surface of rear section at h/D=0.75 for α=0° and 4° and at h/D=1.00 for α=8°. At α=12° early flow separation prevented the interaction of jet-like flow with the trailing edge. As the angle of attack was increased, smaller trapped vortices were observed. As the angle of attack was increased, the saddle point moved closer and below to the trailing edge. Lower immersion ratios caused saddle points to move closer to trailing edge as well as reducing the size of the wake region for α=0° and α=4°. Lower immersion ratios yielded higher drag coefficient values as a result of wavy surface resistance of the free-surface and at an increased angle of attack drag coefficient resulted in higher values as expected. Variations of drag coefficient with immersion ratios and Froude numbers revealed that the effects of free-surface were negligible at h/D≥2.5 for all angles of attacks while their higher values were calculated closer location to the free-surface. In future, CFD results will be compared and validated with the experiments of drag coefficient and PIV measurement.

ACKNOWLEDGEMENTS

ABBREVIATIONS

LES   Large Eddy Simulation

PIV   Particle Image Velocimetry

VOF   Volume of Fluid

NOMENCLATURE

Greek Letters

α   Angle of attack

μ   Dynamic viscosity [kg/ms]

ν   Kinematic viscosity [m2/s]

ρ   Density [kg/m3]

τ   Shear Stress (N/m2)

<ψ>   Time-averaged streamline topologies

Latin Letters

C_D Drag Coefficient [C_D=2F_D/ ρ U_∞^2A]

C_L Lift Coefficient [C_L=2F_L/ ρ U_∞^2A]

C_W Free-surface wave resistance coefficient [C_w=R_w/(1/2) ρ u^{2}s]

D   Diameter [m]

Fr   Froude number [Fr=U_∞/$\sqrt{gh}$]

g   Gravity [m/s^2]

h   Distance between surface and geometry [m]

L   Length [m]

$\dot{m}$ Mass flow rate [kg/s]

Re   Reynolds Number [Re=(U_∞ρL)/μ]

t   Time [s]

U_∞ Freestream velocity [m/s]

<u*>   Time-averaged normalized cross-stream velocity component

u_* Friction velocity

u,v   Streamwise and cross-stream velocity components [m/s]

V   Volume [m^3]

<v*>   Time-averaged normalized cross-stream velocity component

x,y   Streamwise and vertical coordinate directions

y$^+$ Non-dimensional wall distance [y$^+$=yu_*/ ν]

DECLARATION OF ETHICAL STANDARDS

The authors of this article declare that the materials and methods used in this study do not require ethical committee permission and/or legal-special permission.

AUTHORS' CONTRIBUTIONS

Alpaslan KILAVUZ: Investigation, writing and editing of the manuscript.

Muammer OZGOREN: Project director, conceptualization, writing, reviewing and editing of the manuscript.

Tahir DURHASAN: Preparation and comments of figures, review and editing of the manuscript.

Besir SAHIN: Reviewing and proofreading of the manuscript.

Levent Ali KAVURMACIOGLU: Methodology, generating mesh structure and reviewing of the manuscript.

Huseyin AKILLI: Supervision, reviewing and editing of the manuscript

Fuad SARIGIGUZEL: Methodology, software and preparation figures.

CONFLICT OF INTEREST

There is no conflict of interest in this study.

REFERENCES

[1] Givler, R. C., Gartling, D. K., Engelman M. S. and Haroutunian V., "Navier-Stokes simulations of flow past three-dimensional submarine models", *Computer Methods in Applied Mechanics and Engineering*, 87, 175-200, (1991).

[2] Reichl, P., Hourigan, K. and Thompson, K., "The unsteady wake of a circular cylinder near a free surface", *Flow Turbulence and Combustion*, 71, 347-359, (2003).

[3] Evans, J. and Nahon, M., "Dynamics modeling and performance evaluation of an autonomous underwater vehicle", *Ocean Engineering*, 31, 1835-1858, (2004).

[4] Alvarez, A., Bertram, V. and Gualdesi, L., "Hull hydrodynamic optimization of autonomous underwater vehicles operating at snorkeling depth", *Ocean Engineering*, 36, 105-112, (2009).

[5] Jagadeesh, P. and Murali, K., "RANS predictions of free surface effects on axisymmetric underwater body", *Engineering Applications of Computational Fluid Mechanics*, 4:2, 301-313, (2010).

[6] Jagadeesh, P., Murali, K. and Idichandy, V.,"Experimental Investigation of Hydrodynamic Force Coefficients Over AUV Hull Form", *Ocean Engineering*, 36 (1), 113-118, (2009).

[7] Ozgoren M., Dogan, S., Okbaz, A., Sahin, B. and Akıllı, H., "Experimental investigation of turbulence flow structures occurred interactions between sphere and free surface ", *18. Congress on Thermal Science and Technology*, Zonguldak, 141-146, (2011).

[8] Hassanzadeh, R., Sahin, B. and Ozgoren, M., "Large eddy simulation of free-surface effects on the wake structures downstream of a spherical body", *Ocean Engineering*, 54, 213-222, (2012).

[9] Dogan, S., Ozgoren M., Okbaz, A., Sahin, B. and Akilli, H., "Investigation of interactions between a sphere wake and free surface", *Journal of the Faculty of Engineering and Architecture of Gazi University*, 3,33, 1123-1133, (2018).

[10] Nematollahi A., Dadvand A. and Dawoodian M., "An Axissymmetric Underwater Vehicle-Free Surface Interaction: A Numerical Study", *Ocean Engineering*, 96, 205-21, (2015).

[11] Goktepeli I., Ozgoren M., Yagmur S., Kose F., Kavurmacioglu L., 2015, Numerical Flow Characteristics Investigation Around the Semi Elliptic/Elliptic Nose-Shaped Cylindrical Geometries, *Congress on Thermal Science and Technology*, Balıkesir, 1368-1376, (2015).

[12] Salari, M., & Rava, A., "Numerical investigation of hydrodynamic flow over an AUV moving in the water-surface vicinity considering the laminar-turbulent transition", *Journal of Marine Science and Application,* 16(3), 298-304, (2017).

[13] Javanmard, E., & Mansoorzadeh, S., "A Computational Fluid Dynamics Investigation on the Drag Coefficient Measurement of an AUV in a Towing Tank", *Journal of Applied Fluid Mechanics*, 12(3), 947-959, (2019).

[14] Tian, W., Song, B., & Ding, H., "Numerical research on the influence of surface waves on the hydrodynamic performance of an AUV". *Ocean Engineering*, 183, 40-56, (2019).

[15] Kilavuz, A., "Investigation of Flow Characteristics Occuring by Interactiong of Different Torpedo-Like Geometries with a Free Water Surface", *MSc Thesis*, Çukurova University,Institute of Natural and Applied Sciences, (2020).

[16] Kilavuz, A., Ozgoren, M., Durhasan, T., Sahin, B., Kavurmacioglu, L., Akilli, H., Sarigiguzel, F., "Analysis of Attack Angle Effect on Flow Characteristics Around Torpedo-Like Geometry Placed Near the Free-Surface via CFD", *Congress on Thermal Science and Technology*, Kocaeli, 724-732, (2019).

[17] ANSYS Inc., "Large Eddy Simulation (LES) Model", Anysys Fluent User's Guide 6.3, (2009).

[18] ANSYS Inc., "Volume of Fluid (VOF) Model Theory", Anysys Fluent User's Guide 12.0, (2009).

[19] Myring, D. F.,"A theoretical study of body drag in subcritical axisymmetric flow", *The Aeronautical Quarterly*, 27(3), 186-194, (1976).

[20] Barros, E. A., Dantas, J. L., Pascoal, A. M., & de Sá, E.,"Investigation of normal force and moment coefficients for an AUV at nonlinear angle of attack and sideslip range", *IEEE Journal of Oceanic Engineering*, 33(4), 538-549, (2008).

[21] Gao T., Wang Y., Pang Y., and J. Cao,"Hull shape optimization for autonomous underwater vehicles using CFD", *Engineering Applications of Computational Fluid Mechanics*,10 (1), 599–607, (2016).

[22] Sousa J.V.N. , Macêdo A. R. L., Amorim J.W. F. , Lima A. G. B.,"Numerical Analysis of Turbulent Fluid Flow and Drag Coefficient for Optimizing the AUV Hull Design", *Open Journal of Fluid Dynamics*, 4, 263-277, (2014).

[23] Alam K., Ray T., Anavatti S.G., 2014, "Design and construction of an autonomous underwater vehicle", *Neurocomputing*, 142, 16–29, (2014).

[24] ANSYS Inc., Anysys Fluent User's Guide 12.0, (2009).

[25] Anonymous,2020b,<https://www.simscale.com/forum /t/what-is-y-yplus/82394>,accessed: 25.05.2020.

[26] Yagmur S, Goktepeli I, Ozgoren M, Kose F. and Kavurmacioglu L., "Numerical Investigation of Attack Angle Effect on a Torpedo-Like Geometry", *1st International Mediterranean Science and Engineering Congress*, Adana, 4907-4915, (2016).

[27] Yagmur S, Goktepeli I, Ozgoren M., Kose F. and Kavurmacioglu L., "Investigation On Hydrodynamic Characteristics of a Torpedo-Like Geometry via Different Turbulence Models and PIV", *The Second Global Conference on Innovation in Marine Technology and the Future of Maritime Transportation*, Bodrum, 660-673, (2016).

[28] C. Yunus A., C. John M., "Fluid Mechanics: *Fundamentals and Applications*, McGraw-Hill Education, (2018).

[29] Ahmadzadehtalatapeh M., Mousavi M., "A Review on the Drag Reduction Methods of the Ship Hulls for Improving the Hydrodynamic Performance", *International Journal of Maritime Technology*, 4, 51-64, (2015).